Available online at www.sciencedirect.com
ScienceDirect
Journal of Pharmaceutical and Biomedical Analysis 44 (2007) 796–801
JOURNAL OF PHARMACEUTICAL AND BIOMEDICAL ANALYSIS
www.elsevier.com/locate/jpba

Study on the interaction between salicylic acid and catalase by spectroscopic methods

Yunhua Wu *

Key Lab for Biotechnology of National Commission for Nationalities, College of Life Science, The South Central University for Nationalities, Wuhan 430074, PR China

Received 26 January 2007; received in revised form 15 March 2007; accepted 19 March 2007
Available online 25 March 2007

Abstract

The interaction between catalase (CAT) and salicylic acid (SA) was studied by fluorescence and UV–vis spectroscopic techniques. The quenching mechanism of fluorescence of BSA by CAT was discussed to be a static quenching procedure. The number of binding sites n and apparent binding constant K was measured by fluorescence quenching method. The thermodynamics parameter ΔH, ΔG, ΔS were calculated. The results indicate the binding reaction was both entropy-driven and the enthalpy-driven, and the hydrogen bond and van der Waals force played major role in the binding reaction. The binding sites of SA with CAT was investigated to be approached the microenvironment of Trp by the synchronous fluorescence spectrometry. The distance r between donor (CAT) and acceptor (SA) was obtained according to Förster theory of non-radioactive energy transfer.

Keywords: Salicylic acid; Catalase; Synchronous fluorescence; Spectrometric methods

1. Introduction

Salicylic acid (SA) belongs to a group of plant phenolics widely distributed in plants and is now considered as a hormone-like substance, which plays an important role in the regulation of plant growth and development (transpiration, stomatal closure, seed germination, fruit yield, glycolysis, flowering and heat production [1,2]). In recent years, SA has received particular attention because its accumulation is essential for expression of multiple modes of plant disease resistance. A large body of evidence has accumulated suggesting that H_2O_2 accumulation is essential for expression of multiple modes of plant disease resistance. Exogenous SA treatments can induce an increase in H_2O_2 levels in plant tissues. A direct physiological effect of SA is the alteration of antioxidant enzyme activities in vivo. Certain enzymes (guaiacol peroxidase and glutathione reductase) were activated by SA treatment, while catalase was found to be inhibited [3,4]. Catalase seems to be a key enzyme in SA-induced stress tolerance. The heat tolerance in mustard and tobacco and the chilling tolerance in maize were accompanied by decreased catalase activities. SA was proven to bind directly to the catalase enzyme, thereby inhibiting its activity in tobacco [5,6] and other plant species [7].

Catalase is still the subject of many mechanistic investigations. There is increasing evidence that catalase is a major factor in a variety of pathological states such as cancer, diabetes, aging, and oxidative stress [8,9]. Inactivation and reactivation of catalase *in vivo* and *in vitro* are far from being fully understood. Numerous recent publications suggest new approaches regarding *in vitro* assays and inhibition studies on catalase [8–10]. In the Durner's report [11], he provides new insights into SAs effects on catalase. SA acts as an electron donor for the peroxidative cycle of both plant and animal catalases. As such, it can protect as well as inhibit catalase activity, depending on the concentration of H_2O_2. It is hypothesized that, in healthy tissue of infected leaves where H_2O_2 levels are low, SA inhibits catalase, which could lead to activation of defense-related genes. In contrast, in infected cells and in tissue immediately adjacent to necrotizing cells, where high levels of H_2O_2 and other reactive oxygen species are produced, SA protects catalase from inactivation. To our knowledge, however, to date the interaction parameters between SA and CAT in vitro has not been investigated. Fluorescence and UV–vis absorption spectroscopy are powerful tools for the study of the reactions of chemical

* Tel.: +86 27 6240 6765; fax: +86 27 6784 2689.
E-mail address: yunhuawu@yahoo.com.cn.

0731-7085/$ – see front matter © 2007 Elsevier B.V. All rights reserved.
doi:10.1016/j.jpba.2007.03.016

and biological systems since it allows non-intrusive measurements of substances in low concentration under physiological conditions.

The aim of our work was to determine the affinity of SA to CAT, and to investigate the thermodynamics of their interaction. To resolve this problem, the UV–vis and fluorescent properties of CAT, as well as SA, were investigated.

2. Experimental

2.1. Apparatus

All fluorescence measurements were made with a Hitachi F-2500 spectrofluorimeter (Tokyo, Japan) equipped with a 1 cm quartz cell and a thermostat bath. A UV-757CRT visible ultraviolet spectrophotometer (Shanghai Precision & Scientific Instrument Co. Ltd., China) equipped with 1.0 cm quartz cells was used for scanning the UV spectrum. All pH measurements were made with a pHs-3 digital pH-meter (Shanghai Lei Ci Device Works, Shanghai, China) with a combined glass electrode.

2.2. Reagents

All starting materials were analytical reagent grade and double distilled water was used for all the measurements. 5.0×10^{-3} mol L^{-1} SA was prepared. Catlase (2000–5000 U/mg, from Bovine Liver, Sigma) was directly dissolved in water to prepare stock solutions (3.0×10^{-3} mol L^{-1}) and then stored at 4 °C; 0.2 mol L^{-1} phosphate buffer solution of pH 7.2 was prepared.

2.3. Procedures for fluorescence spectrum measurements

To a 10 mL standard flask, appropriate amount of SA solution, CAT, proper amount of phosphate buffer were added, and then shaken. Fluorescence quenching spectra of catalase were obtained at excitation and emission wavelengths of $\lambda_{ex} = 280$ nm and $\lambda_{em} = 300$–500 nm. An excitation wavelength of 280 nm was chosen since it provides excitation of CAT with a strong fluorescence emission. Synchronous fluorescence spectrometry of Tyr and Trp were obtained by setting $\Delta\lambda = 20$ nm and $\Delta\lambda = 80$ nm, respectively. The excitation and emission slit widths were set at 10.0 nm. Appropriate blanks corresponding to the buffer were subtracted to correct background fluorescence. The absorption spectra of CAT, SA and their mixture were performed at room temperature.

3. Results and discussion

3.1. Binding constant and binging numbers of SA and CAT

3.1.1. UV–vis absorption spectra

Fig. 1 shows the UV–vis absorption spectra of CAT and its mixture with SA in phosphate buffer (pH 7.2), which is obtained by keeping the CAT concentration constant and changing the SA concentration. In the wavelength range from 350 to 550 nm, CAT has a maximum absorption at 402 nm (curve a) and SA has no any absorption (curve d). With the addition of SA, the maximum absorption of CAT at 402 nm decreases and the maximum absorption peak is not changed (curve b and c). The change of absorption spectra of CAT with the addition of SA indicates that there are binding interactions between CAT and SA [12]. The reproducibility of the curves in Fig. 1 was also investigated. Keeping the concentration of SA and CAT constant, the RSD of the value of absorbance decrease was obtained as 2.03% for ten replicate measurements.

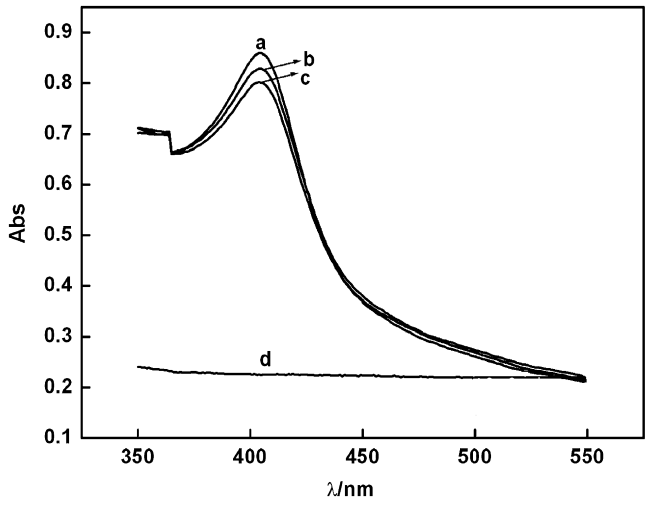

Fig. 1. Absorption spectra of SA bound to CAT at pH 7.2. $C_{CAT} = 3 \times 10^{-4}$ mol L^{-1}, $C_{SA} = 0$ mol L^{-1} (a); $C_{SA} = 1 \times 10^{-5}$ mol L^{-1} (b); $C_{SA} = 2 \times 10^{-5}$ mol L^{-1} (c); absorption spectra of SA only, $C_{SA} = 1 \times 10^{-4}$ mol L^{-1} (d).

3.1.2. Fluorescence spectrometry

Fluorescence spectroscopy is the most favorable technique in the study of molecular interactions, in particular because of its high sensitivity, and multiplicity of measurable parameters. To find the binding of SA to CAT in detail, fluorescence experiments were carried out. The fluorescence quenching spectra of CAT at various concentrations of SA are shown in Fig. 2. By fixing the excitation wavelength at 280 nm, CAT and SA had a strong fluorescence emission band at 311 nm and 410 nm, respectively. The fluorescence intensity of CAT decreased regularly, and the emission wavelength of CAT had no change with increasing SA concentration. Moreover, the occurrence of an isosbestic point at 345 nm was observed, indicating that a SA–CAT complex was formed, which could quench the fluorescence of CAT.

Quenching can occur by different mechanisms, which usually classified as dynamic quenching and static quenching. Dynamic and static quenching can be distinguished by their differing dependence on temperature and viscosity. Higher temperatures result in faster diffusion and hence larger amounts of collisional quenching. Higher temperatures will typically result in the dissociation of weekly bound complexes, and hence smaller amounts of static quenching. Thus, the quenching rate constants decrease with increasing temperature for static quenching, but the reverse effect is observed for the case of dynamic quenching.

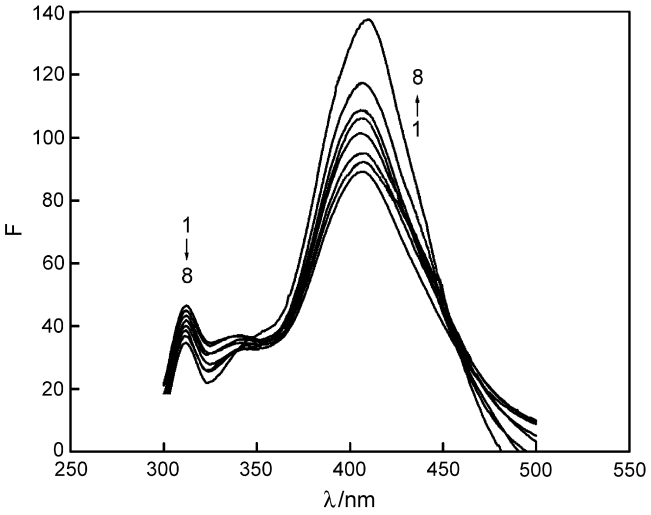

Fig. 2. Effect of SA on fluorescence spectra of CAT. C_{SA} (mol L^{-1}): (1) 2×10^{-6}; (2) 4×10^{-6}; (3) 6×10^{-6}; (4) 8×10^{-6}; (5) 1×10^{-5}; (6) 1.2×10^{-5}; (7) 1.4×10^{-5}; (8) 1.6×10^{-5}. $C_{CAT} = 1 \times 10^{-6}$ mol L^{-1}, $\lambda_{ex} = 280$ nm, pH 7.2, 25 °C.

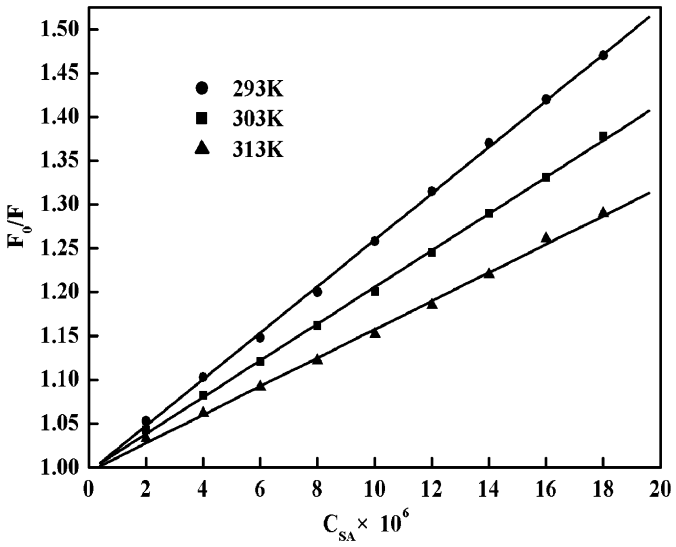

Fig. 3. The Stern–Volmer curves of quenching of CAT with SA at various temperatures. Others are the same as those in Fig. 2.

In order to confirm this point, the procedure was assumed to be dynamic quenching. The quenching equation is presented by:

$$\frac{F_0}{F} = 1 + K_q \tau_0 [Q] = 1 + K_{SV}[Q] \quad (1)$$

where F and F_0 are the fluorescence intensities with and without quencher, K_q the quenching rate constant of the biomolecule, K_{SV} the Stern–Volmer quenching constant, τ_0 the average lifetime of the biomolecule without quencher and $[Q]$ is the concentration of quencher. Obviously:

$$K_q = \frac{K_{SV}}{\tau_0} \quad (2)$$

The possible quenching mechanism can be interpreted by the fluorescence quenching spectra of CAT and the $F_0/F \sim C$ (Stern–Volmer) curves of CAT with SA at different temperatures (293 K, 303 K and 313 K) as shown in Fig. 3. The results of linear regressions of Fig. 3 are: $F_0/F = 0.99544 + 16200$ [SA] at 313 K, $F_0/F = 0.99671 + 20910$ [SA] at 303 K, and $F_0/F = 0.99483 + 26480$ [SA] at 293 K, respectively. Because the fluorescence lifetime of the biopolymer τ_0 is 10^{-8} s^{-1} [13], the corresponding Stern–Volmer quenching constant, K_{SV}, at different temperatures are shown in Table 1. According to the Eq. (2), the quenching constant K_q was obtained to be 1.62×10^{12} L mol^{-1} s^{-1}, 2.091×10^{12} L mol^{-1} s^{-1} and 2.648×10^{12} L mol^{-1} s^{-1} at 313 K, 303 K and 293 K, respectively. However, the maximum scatter collision quenching constant K_q of various quenchers with the biopolymer is 2×10^{10} L mol^{-1} s^{-1} [14]. Obviously, the rate constant of CAT quenching procedure initiated by SA is greater than K_q of the scatter procedure. These results indicate that the probable quenching mechanism of fluorescence of CAT by SA is not a dynamic quenching procedure but a static quenching procedure, because the K_{SV} decreased with the temperature rising.

When small molecules bind independently to a set of equivalent sites on a macromolecule, the values of K_A and n can be determined according to the method described by Liu and coworkers [15] using the equation:

$$\log \frac{F_0 - F}{F} = \log K_A + n \log [SA] \quad (3)$$

where K_A is the binding constant of SA and CAT, n the binding numbers, which can be determined by the intercept and slope of the plot $\log(F_0 - F)/F \sim \log[SA]$ as shown in Fig. 4, respectively. Table 2 gives the results at different temperatures analyzed

Table 2
Binding constant K_A and binding sites n at different temperatures

T (K)	$K_A \times 10^4$ (L mol^{-1})	n	R^a	S.D.[b]
293	4.457	1.06	0.9963	0.030
303	4.435	1.02	0.9994	0.011
313	4.169	0.99	0.9991	0.014

[a] Linear correlated coefficient.
[b] Standard deviation.

Table 1
Thermodynamic parameters of SA–CAT system

T (K)	$K_{SV} \times 10^{-4}$ (L mol^{-1})	R^a	S.D.[b]	ΔG (kJ mol^{-1})	ΔH (kJ mol^{-1})	ΔS (J mol^{-1} K^{-1})
293	2.648	0.9958	0.025	−12.19		
303	2.091	0.9963	0.021	−11.94	−19.42	−24.79
313	1.62	0.9972	0.018	−11.69		

[a] Linear correlated coefficient.
[b] Standard deviation.

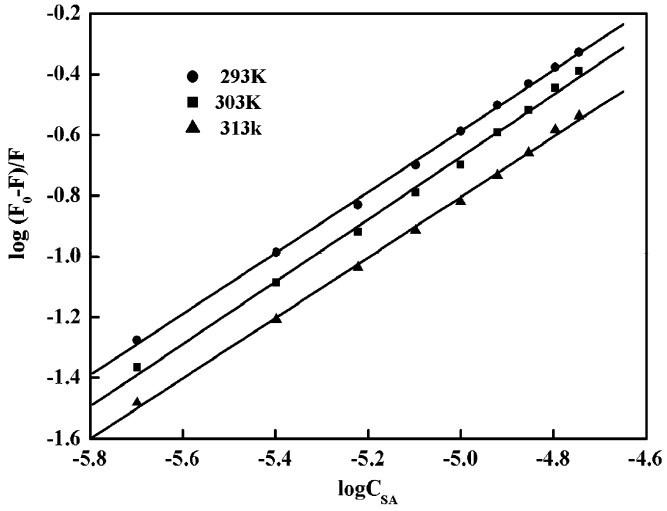

Fig. 4. The plot of $\log(F_0 - F)/F$ vs. log[SA] for quenching of CAT with SA at various temperatures. Others are the same as those in Fig. 2.

in this way for CAT. The linear correlated coefficients (R) are larger than 0.99, and the standard deviation is less than 0.04, indicating that the assumptions underlying the derivation of Eq. (4) are satisfied. Table 2 shows the results of K_A values did not show a great sensitivity to temperature over the temperature range studied and n is almost constant, which maybe indicates that there is Oxaprozin-E molecular binding with BSA according to molar scale 1:1 and forming a stable complex relatively. It shows that the binding constant between SA and CAT is great, thus, SA bound to CAT strongly.

3.2. Binding site and binging distance of SA and CAT

3.2.1. Synchronous fluorescence spectrometry

Fluorescence spectrometry is the often used and effective method to study the interaction of protein with exogenous substances [16]. Similar to other proteins, the Tyr, Trp and Phe residues of CAT result in its endogenesis fluorescence. The fluorescence spectrum of these amino acid residues overlaps each other and it is difficult to differentiate them by common fluorescence spectrometric method. In our experiment, the interaction of SA with CAT was investigated by synchronous fluorescence spectrometry. In Figs. 1, 2 and 5 are the synchronous fluorescence spectrometry of Tyr, Trp residues, respectively, 1′, 2′ are the synchronous fluorescence spectrometry of Tyr, Trp residues after addition with SA, respectively. It is observed that SA had little effect of the fluorescence of Tyr (270–300 nm), but that from Trp was virtually completely eliminated (370–400 nm). This suggests SA binding to CAT affects the microenvironment of Trp but not Tyr.

3.2.2. Energy transfer between SA and CAT

According to Förster's non-radiative energy transfer theory [17], the energy transfer will happen under the conditions: (i) the donor can produce fluorescence light, (ii) fluorescence emission spectrum of the donor and UV absorption spectrum of the acceptor have more overlap and (iii) the distance between the donor

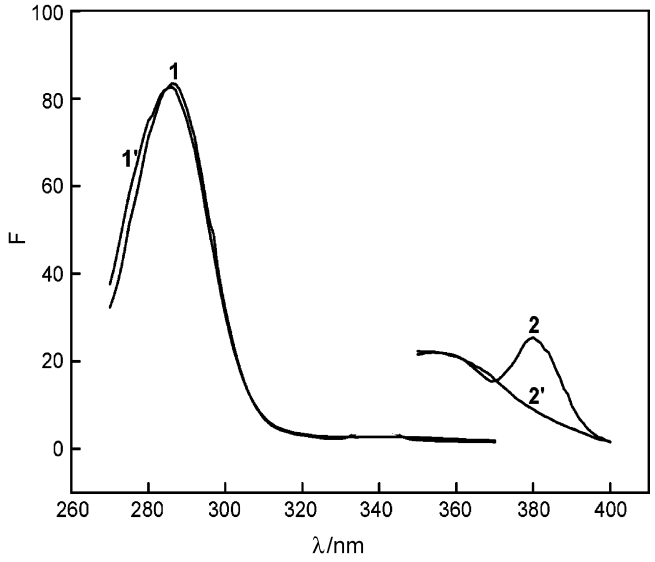

Fig. 5. Synchronous fluorescent spectra of CAT in the presence of SA (1′, 2′, $C_{SA} = 1 \times 10^{-6}$ mol L^{-1}, curve 1′, 2′) and absence of SA (curve 1, 2). $\Delta\lambda = 20$ nm (curve 1, 1′); $\Delta\lambda = 80$ nm (curve 2, 2′).

(CAT) and the acceptor (SA) is lower than 7 nm. The fluorescence quenching of CAT after binding with SA indicated that the energy transfer between SA and CAT occurred. The overlap of the UV absorption spectrum of SA with the fluorescence emission spectrum of CAT is shown in Fig. 6. The efficiency of energy transfer, E, was studied according to Förster's energy transfer theory [17]. The efficiency of energy transfer, E, is calculated using the equation:

$$E = \frac{R_0^6}{R_0^6 + r^6} = 1 - \frac{F}{F_0} \tag{4}$$

where F and F_0 are the fluorescence intensities of CAT in the presence and absence of SA, r the distance between acceptor and donor and R_0 is the critical distance when the transfer efficiency

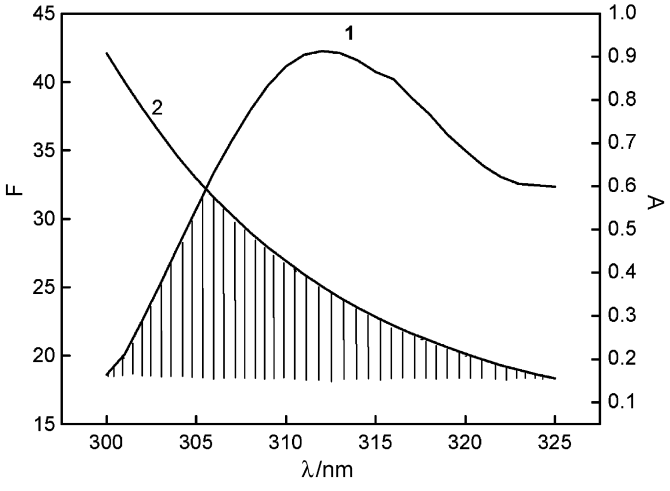

Fig. 6. The overlap of the UV spectrum of SA with the fluorescence emission spectrum of CAT. (1) The fluorescence spectrum of CAT, $C_{CAT} = 1 \times 10^{-6}$ mol L^{-1}, F is the fluorescence intensity; (2) the UV absorbance spectrum of SA, $C_{SA} = 1 \times 10^{-6}$ mol L^{-1}, A is the UV absorption intensity of SA.

is 50%. The value of R_0 is calculated using the equation:

$$R_0^6 = 8.8 \times 10^{-25} k^2 \varphi n^{-4} J \quad (5)$$

where k^2 is the spatial orientation factor of the dipole, n the refractive index of the medium, φ the overlap integral of the fluorescence emission spectrum of the donor and J is the overlap integral of the fluorescence emission spectrum of the donor and the absorption spectrum of the acceptor. Therefore:

$$J = \frac{\sum F(\lambda)\,\varepsilon(\lambda)\lambda^4\,\Delta\lambda}{\sum F(\lambda)\,\Delta\lambda} \quad (6)$$

where $F(\lambda)$ is the fluorescence intensity of the fluorescent donor at wavelength λ, $\varepsilon(\lambda)$ is the molar absorption coefficient of the acceptor at wavelength λ. J can be evaluated by integrating the spectra in Fig. 6. It has been reported for CAT that, $k^2 = 2/3$, $\varphi = 0.118$, $n = 1.336$ [18]. Based on these data, we calculated that $R_0 = 3.22$ nm and $r = 2.62$ nm. The donor-to-acceptor distance, $r < 7$ nm indicated that the energy transfer from CAT to SA occurs with high possibility. Calculations suggest non-radiative energy transfer between SA and CAT, indicating again the static quenching interaction between CAT and SA.

3.3. Binding mode

Considering the dependence of binding constant on temperature, a thermodynamic process was considered to be responsible for the formation of the complex. Therefore, the thermodynamic parameters dependent on temperatures were analyzed in order to further characterize the acting forces between SA and CAT. The acting forces between a small molecule substance and macromolecule mainly include hydrogen bond, van der Waals force, electrostatic force, hydrophobic interaction force and so on. The thermodynamic parameters, enthalpy ΔH, entropy ΔS and free energy change ΔG, are the main evidences to estimate the binding mode. A plot of ln K versus $1/T$ gives a straight line according to the van't Hoff equation:

$$\ln K = -\frac{\Delta H}{RT} + \frac{\Delta S}{R} \quad (7)$$

where constants K are analogous to the Stern–Volmer quenching constants K_{SV} at the corresponding temperature [19] (the temperatures used were 293 K, 303 K and 313 K). The free energy change ΔG is estimated from the following relationship:

$$\Delta G = \Delta H - T\,\Delta S \quad (8)$$

Fig. 7 was obtained by plotting the values of ln K_{SV} versus $1/T$. The value of ΔG was further calculated based on Eq. (8). The results are shown in Table 1. From Table 1, it can be seen that the negative sign for free energy ΔG means that the interaction process is spontaneous. The negative enthalpy ΔH and entropy ΔS values of the interaction of SA and CAT, indicate that the binding is both entropy-driven and the enthalpy-driven, the hydrogen bond and van der Waals force played major role in the reaction [20].

From Eckelt's report [21], it is know that there are five Trp residues in the enzyme and Trp is not resent in the active site

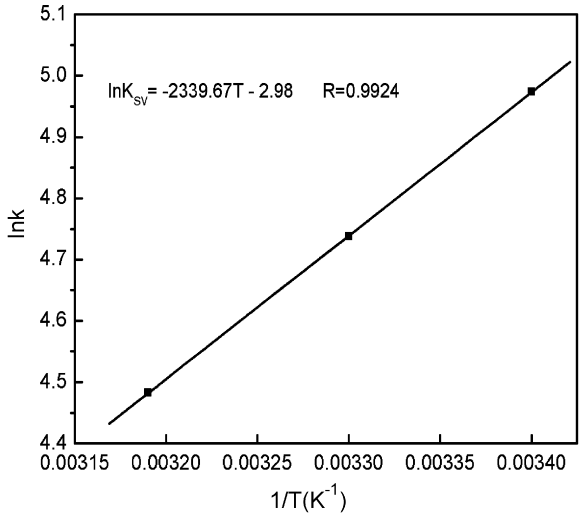

Fig. 7. van't Hoff plot for the binding of SA to CAT.

of the enzyme. Among the five Trp residues, the region, which Trp-302 lies in is the most hydrophobic. The hydrophobic environment is in favor of the formation of hydrogen bond between SA and CAT. Hence, Trp-302 is the main binding site for SA in CAT. Trp-302 maybe play a role in keeping the conformation of the enzyme. Thus, it is hypothesized that, when SA and Trp-302 bound with hydrogen bond, it destroys the conformation of the enzyme, leads to changes in enzymatic activity. Hydrogen peroxide can affect the binding between SA and CAT via interferring the formation of hydrogen bond.

4. Conclusions

The binding of salicylic acid (SA) to catalase (CAT) in aqueous solution was studied by fluorescence and UV–vis spectroscopic methods. The results show that SA has a strong ability to quench the CAT fluorescence mainly through a static quench procedure. The binding constant K and the number of binding site n were calculated according to the fluorescence quenching results. Based on the mechanism of energy transfer, the donor–acceptor distance of the SA and CAT was calculated as 2.62 nm. It is inferred that the binding site of SA to CAT is approached the microenvironment of Trp residues of CAT by synchronous fluorescence spectrometry.

Acknowledgement

This work was supported by the Natural Science Foundation of The South Central University for Nationalities (YZZ-06-008).

References

[1] I. Raskin, Annu. Rev. Plant Physiol. Plant Mol. Biol. 43 (1992) 439–463.
[2] D.F. Klessig, J. Malamy, Plant Mol. Biol. 26 (1994) 1439–1458.
[3] J.F. Dat, H. Lopez-Delgado, C.H. Foyer, I.M. Scott, Plant Physiol. 116 (1998) 1351–1357.
[4] T. Janda, G. Szalai, I. Tari, E. Paídi, Planta 208 (1999) 175–180.
[5] Z. Chen, J.R. Ricigliano, D.F. Klessig, Proc. Natl. Acad. Sci. U.S.A. 90 (1993) 9533–9537.

[6] U. Conrath, Z. Chen, J.R. Ricigliano, D.F. Klessig, Proc. Natl. Acad. Sci. U.S.A. 92 (1995) 7143–7147.
[7] P. Sáchez-Casas, D.F. Klessig, Plant Physiol. 106 (1994) 1675–1679.
[8] J. Durner, D.F. Klessig, Proc. Natl. Acad. Sci. U.S.A. 92 (1995) 11312–11316.
[9] R.J. Feuers, F.M. Patillo, C.K. Osborn, K.L. Adams, D. DeLuca, W.G. Smith, Free Radic. Biol. Med. 15 (1993) 223–226.
[10] D.W.A. Hook, J.J. Harding, FEBS Lett. 382 (1996) 281–284.
[11] J. Durner, D.F. Klessig, J. Biol. Chem. 271 (1996) 28492–28501.
[12] D. Leis, S. Barbosa, D. Attwood, P. Taboada, V. Mosquera, J. Phys. Chem. B 106 (2002) 9143–9150.
[13] J.R. Lakowicz, G. Weber, Biochemistry 12 (1973) 4161–4170.
[14] W.R. Ware, Phys. Chem. 66 (1962) 445–458.
[15] J. Kang, Y. Liu, M. Xie, S. Li, M. Jiang, Y. Wang, Biochim. Biophys. Acta 1674 (2004) 205–214.
[16] J.M. Anni, K.A.S. Vanderkooi, T. Yonetani, S.C. Hopkins, L. Herenyi, J. Fidy, Biochemistry 33 (1994) 3475–3486.
[17] L.A. Sklar, B.S. Hudson, R.D. Simoni, Biochemistry 16 (1977) 5100–5106.
[18] M.M. Yang, P. Yang, L.W. Zhang, Chin. Sci. Bull. 39 (1994) 31–35.
[19] C.B. Murphy, Y. Zhang, T. Troxler, V. Ferry, J.J. Martin, W.E. Jones, J. Phys. Chem. B 108 (2004) 1537–1543.
[20] P.D. Ross, S. Subramanian, Biochemistry 20 (1981) 3096–3102.
[21] V.H.O. Eckelt, E. Liebau, R.D. Walter, K. Henkle-Du¨hrsen, Mol. Biochem. Parasit. 95 (1998) 203–214.